Gold Bull (2013) 46:283–290
DOI 10.1007/s13404-013-0127-4

ORIGINAL PAPER

Nanostructured and nanopatterned gold surfaces: application to the surface-enhanced Raman spectroscopy

A. Bouvrée · A. D'Orlando · T. Makiabadi · S. Martin · G. Louarn · J. Y. Mevellec · B. Humbert

Published online: 11 December 2013

Abstract Surface-enhanced Raman spectroscopy (SERS) has enormous potential for a range of applications where high sensitivity needs to be combined with good discrimination between molecular targets. However, the SERS technique has trouble finding its industrial development, as was the case with the surface plasmon resonance technology. The main reason is the difficulty to produce stable, reproducible, and highly efficient substrates for quantitative measurements. In this paper, we report a method to obtain two-dimensional regular nanopatterns of gold nanoparticles (AuNPs). The resulting patterns were evaluated by SERS. Our bottom-up strategy was divided into two steps: (a) nanopatterning of the substrate by e-beam lithography and (b) electrostatic adsorption of AuNPs on functionalized substrates. This approach enabled us to highlight the optimal conditions to obtain monolayer, rows, or ring of AuNPs, with homogeneous distribution and high density (800 AuNPs/μm^2). The nanostructure distributions on the substrates were displayed by scanning electron microscopy and atomic force microscopy images. Optical properties of our nanostructures were characterized by visible extinction spectra and by the measured enhancements of Raman scattering. Finally, we tried to demonstrate experimentally that, to observe a significant enhancement of SERS, the gold diffusers must be extremely closer. If electron beam lithography is a very attractive technique to perform reproducible SERS substrates, the realization of pattern needs a very high resolution, with distances between nanostructures probably of less than 20 nm.

Keywords Surface-enhanced Raman scattering · SERS · Gold nanoparticles · Nanolithography

Electronic supplementary material The online version of this article (doi:10.1007/s13404-013-0127-4) contains supplementary material, which is available to authorized users.

A. Bouvrée · A. D'Orlando · T. Makiabadi · S. Martin · G. Louarn (✉) · J. Y. Mevellec · B. Humbert
Institut des Matériaux Jean Rouxel (IMN), CNRS, Université de Nantes, 2 rue de la Houssinière, BP 32229, 44322 Nantes cedex 3, France
e-mail: guy.louarn@cnrs-imn.fr

Introduction

Assembling nanoparticles into one-, two-, and three-dimensional (1D, 2D, and 3D) arrays attract considerable interest due to their capabilities to generate strong enhancement of electromagnetic field in their near surroundings. This effect is also successfully exploited in Raman spectroscopy, spectroscopy based on the inelastic scattering of a monochromatic light after its interaction with a molecule for instance. Thus, this improvement of the scattering, so called "surface-enhanced Raman scattering," is used for the characterization of materials or more recently in the design of chemical and biochemical sensors [1–3].

Use gold nanoparticles (AuNPs) in aqueous solutions as a way for enhancing Raman scattering was first demonstrated by Creighton et al. [4]. This observed enhancement was due to the interaction of light with metallic nanoparticles. This interaction can be characterized by strong optical resonances due to the excitation of localized surface plasmons [5]. One of the main consequences of plasmon excitation is the high electromagnetic field created at the surface of the nanoparticle. This field is then involved in enhancing the efficiency of Raman process. It should be stressed here that the intensity of the electromagnetic field depends strongly on the nanoparticle size, shape, intercenter distance, and interparticle separation [3].

As a consequence, numerous papers in the literature have developed smart strategies to obtain Raman active substrates, with controlled uniform roughness, or regular nanostructure distributions, with good reproducibility [1–3, 6–8]. In parallel, many approaches were proposed to optimize and control the surface-enhanced Raman scattering efficiency of colloidal AuNPs assembled on substrates into 2D nanostructures [9–19].

Here, we report an alternative procedure for preparing patterned AuNP arrays by combining electron beam lithography which allows control of lateral dimensions down to 20 nm, with self-assembly of silanes on silicon oxide in the micrometer and submicrometer range to direct the AuNPs assembly. A thin polymer layer on a substrate was patterned. The substrate consisted of a polymer relief pattern with exposed substrate regions in between, where (3-aminopropyl)-dimethylethoxysilane (APDMES) was grafted. This substrate could be converted to chemically patterned substrates by removing the polymer template. Then, substrates were used to attach AuNPs by immersion. In this manner, close packing was found on micrometer-sized features, and typical confined particle geometries were observed on submicrometer features. The self-assembly of monolayers of AuNPs on organosilane-coated substrates yields macroscopic surfaces that are highly active for surface-enhanced Raman spectroscopy (SERS) [1, 19]. The strategy delineated herein was the utilization of gold particles to form a well-ordered close-packed 2D nanostructure. Then, thanks to e-beam lithography, given a regular and uniform distribution of lines and circles, we were able to perform a Raman study as a function of the density of nanoparticles adsorbed on the surface and the distance between them.

Materials and methods

Materials

$HAuCl_4$ for AuNPs preparation was bought from Fluka. Other chemical materials, such as sodium citrate (99 %), methanol (99.8 %), APDMES (97 %), and crystal violet (95 %), were purchased from Sigma-Aldrich. Deionized water with a specific resistance of 18 MΩ was used for all preparations.

Instrumentation

Raman spectra were obtained and recorded on a spectrometer multichannel Jobin-Yvon T64000 (HORIBA) spectrometer using the 676.4 nm line of krypton ion lasers. All the experiments were carried out under a confocal microscope to focus the excitation line on the nanopatterned area. A holographic NOTCH filter or a double subtractive stage with gratings with 1,800 grooves mm^{-1} may be used to remove the Rayleigh scattering. A single dispersion stage with 1,800 grooves mm^{-1} grating is placed in front of the detector. The spectral resolution, with excitation at 676.4 nm is 2 cm^{-1}. Raman spectrometer optically conjugated with an Olympus Model BX51 upright microscope was equipped with a motorized XY stage with a step of 80 nm. This setup allowed us to obtain a better lateral spatial resolution than 2 μm [20].

Topographic and morphologic measurements were recorded using scanning electron microscopy (SEM—JEOL JSM 6400 F1) and atomic force microscopy (AFM VEECO Nanoscope IIIa), respectively. The UV-visible absorbance spectra between 200 and 800 nm were obtained with a Varian Cary 2300 spectrometer. The particle size distribution of suspensions was determined by dynamic light scattering using a Zetasizer Nano ZS instrument equipped with a 633-nm He–Ne laser (Malvern Instruments Ltd., Malvern, Worcestershire, UK), which measured the scattered light at an angle of 173° and at a temperature of 25 °C.

Methods

Gold colloids were prepared by modifying the method of citrate thermal reduction reported in [21, 22]. Typically, in the process of thermal reduction, gold colloids were prepared by adding 1 ml of 1 wt% $HAuCl_4$ aqueous solution and 1.5 ml of 38.8 mM sodium citrate aqueous solution drop at drop into 90 ml boiling water under stirring. Then, after 10 min, the solution becomes ruby red signature of the action of citrate ions as both reducer and stabilizer. Indeed, as shown in Fig. 2a, citrate ions are adsorbed on the AuNP, and they modify the charge of AuNPs surface (Zeta potential about −25 mV at pH 3). Finally, the solution was cooled naturally to room temperature with continued stirring. Then, the AuNPs aqueous solution has been concentrated by centrifugation for 10 min (7,800 rpm–10,000*g*). After this centrifugation step, a relatively high concentration of AuNPs has been estimated about 0.96±0.12 nmol/L from optical absorption spectra [23].

Preparation of SERS substrates

First step The electron beam nanopatterned substrates were produced from the technological platforms of the IMCN Institute, UCL, Belgium using the method described in reference [24]. Sketches of the protocol of silanization of patterned lines and rings are presented in Fig. 1. After deposition of PMMA by "spin-coating" on a silicon substrate, different patterns have been formed by electron beam lithography. From this process, the patterns (grooves) in the PMMA provides a very high resolution (about 10 nm) [24, 25] and the film is very resistant to the silanization step. Various geometrical structures were processed, such as concentric rings and line networks. The geometric characteristics of the different samples studied in this work were outlined in the electronic

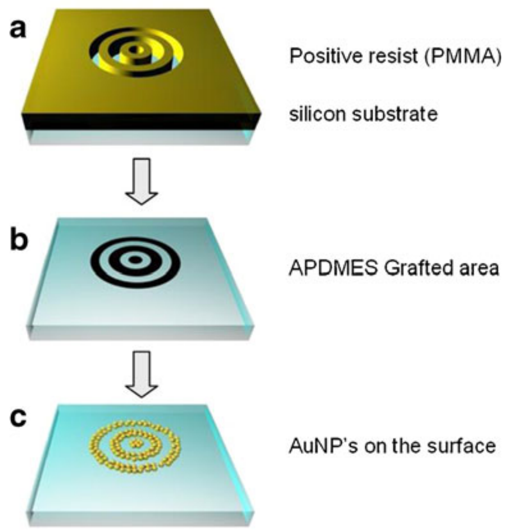

Fig. 1 Sketches of the AuNPs immobilization process on e-beam-patterned substrates (Coll. Alain Jonas, UCL); **a** substrate after e-beam writing step; **b** APDMES-coated substrate step; **c** AuNPs immobilization on APTMS-coated glass or silicon substrates

supplementary material (Fig. S1). Acetone was used to dissolve the PMMA mask at this step.

Second step Immediately after a piranha treatment, the substrate was placed on the sample holder in a Schlenk tube which was heated at 80 °C. The Schlenk tube was closed hermetically with a rubber septum. This tube was then purged several times before to be filled with N_2. APDMES (0.1 mL) was added through the rubber septum in the Schlenk tube, and the system was maintained overnight. At the end, the substrates were placed in a beaker containing dry toluene.

Third step The prepared substrate was then dried for about 30 min at about 100 °C and then rinsed again three times with methanol. Then, the silanized substrate was immersed for different times (also called "soaking times" in the following) in an AuNPs solution which had been concentrated (0.96± 0.12 nmol/L) by centrifugation for 10 min (10,000*g*). Finally, the substrate was rinsed with distilled water.

Raman experiments

SERS spectra of 1 μM crystal violet adsorbed on SERS substrates were carried out after dipping the substrates in a 1-μM dye aqueous solution. In this work, the data were collected immediately after immersion in the dye solution (3 min) without further rinsing, and the main experimental conditions can be summarized as: λ_{exc}=676.4 nm, power of the Raman laser P=0.1 mW, 2 μm diameter spot, and the typical exposure times were 30 s per point. We focused our attention on the C–C in-plane stretching vibration pointed at 1,620 cm^{-1}. The acquisitions were repeated (five to ten Raman spectra for each experimental condition in our present study) at different locations in order to give a full statistical understanding of the enhancement factor.

Results and discussion

The surface morphology and the size of AuNPs were observed by transmission electron microscopy (TEM) and atomic force microscopy (AFM) (height image). In Fig. 2b, the TEM image shows nearly spherical and smooth AuNPs. From the TEM images, the average diameter of particles has been evaluated about 22 nm in complete agreement with the dynamic light scattering results (see supplementary materials, Fig. S2).

Then, these gold particles have been adsorbed on APDMES-coated glass slides thanks to electrostatic interactions between the positively charged amino-terminated groups of APDMES and the citrate anions available on the nanoparticle surface (Fig. 2a) [26]. It should be pointed here that the citrate ions are only adsorbed on the AuNPs; hence, the NPs are electrostatically adsorbed via citrates on the amine groups of silanes (Fig. 2c) [10]. In this way, the electrostatic adsorption implies that the NPs can be desorbed upon changes of ionic strength and pH. In order to prevent the desorption of AuNPs and according to the reference [19], significant attention has been paid to the drying after silanization (30 min, 100 °C) and after nanoparticles immobilization (10 min, 90 °C). This protocol is a needful step to prepare stable SERS active surfaces and to increase the reproducibility and stability of the surface. This drying probably reduced hydration of citrate anions adsorbed on the gold surface, and it allows a closer interaction of neighboring nanoparticles in the monolayer structure [19]. However, the stability and the regularity of the NP layers at different media and in presence of different chromophores will have to be considered carefully before each experiment.

Figure 2d, e shows the SEM and AFM (height) images of the AuNPs adsorbed onto modified solid substrates after soaking in AuNPs aqueous solution at 40 °C for 30 min. AuNPs in rather well-defined 2D structures were successfully constructed on glass or silicon slides. In fact, different temperatures have been tested from 20 to 50 °C. As presented in Fig. S3 (in the supplementary materials) at 50 °C and higher, a homogeneous distribution of AuNPs on the surface was not obtained. Indeed, a higher temperature increases the mobility of the nanoparticles on the surface, and the interparticle repulsion was screened. In the same way, for low soaking times, the particles are isolated but too far to induce high local electric field. After 30 min at 40 °C, the film demonstrated a close-packed colloid monolayer, while aggregation started afterwards (after 60 min and more). Thus, 40 °C and 30 min were fixed in our soaking process. In these conditions, the particles were closely spaced, and the film of AuNPs was relatively

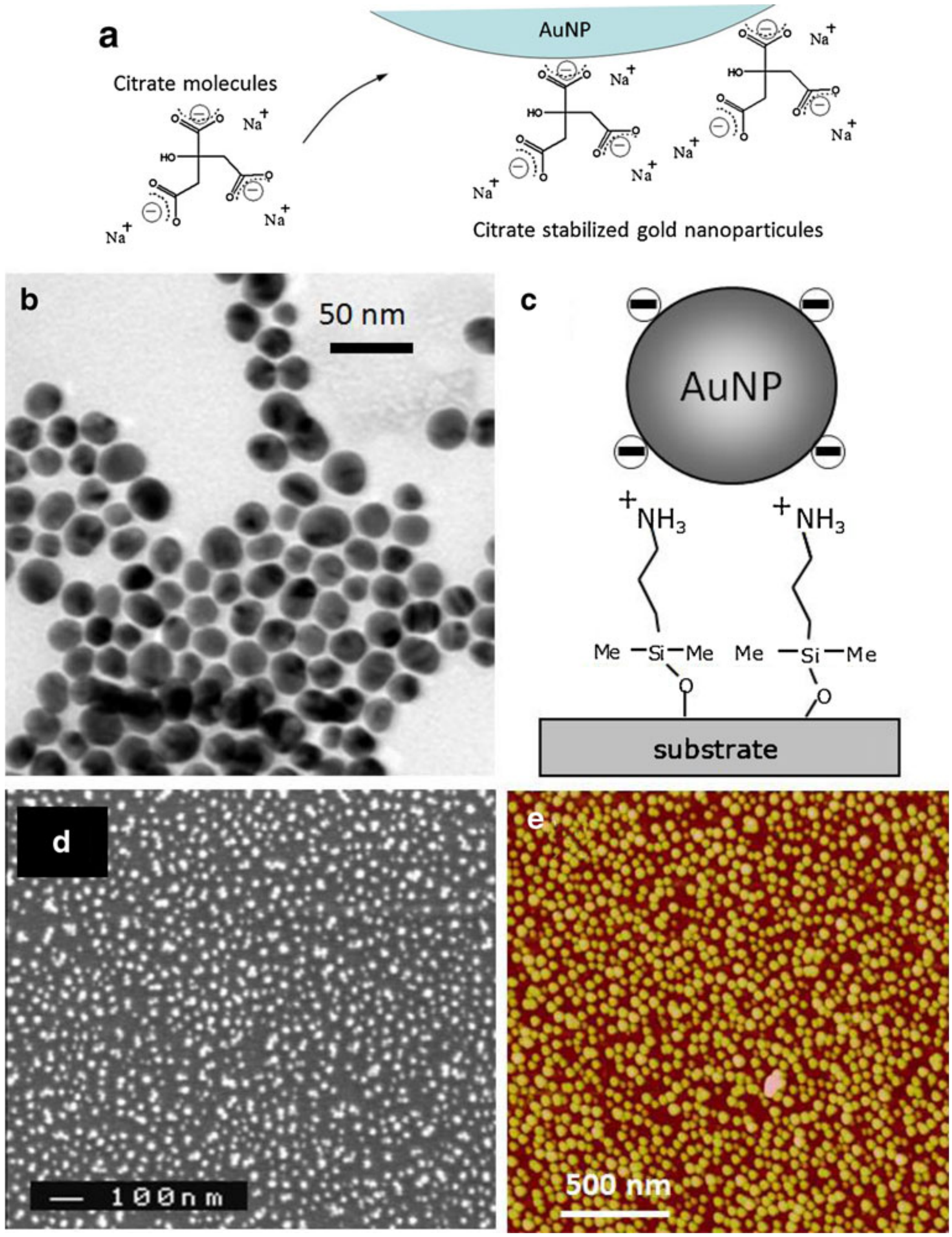

Fig. 2 **a** Schematic representation of the electrostatic adhesion process of citrate occurring during the synthesis of AuNPs; **b** TEM image of the AuNPs obtained by reducing HAuCl4 with Na-citrate; **c** schematic representation of AuNPS immobilization on APDMES-coated glass substrates; **d** SEM image and **e** tapping mode AFM image of immobilized AuNPs on APDMES-coated glass prepared by soaking the substrate in an AuNPs aqueous solution (0.96± 0.12 nmol/L) for 30 min and at 40 °C

uniform with a rather good regularity over wide areas. These observations confirmed previous studies [27–29].

UV-visible adsorption spectra of colloidal suspension and substrates

The absorbance of the gold nanoparticle samples was measured by optical spectroscopy. A typical UV-visible adsorption spectrum of the gold colloidal solution is shown in Fig. 3a(a). The adsorption spectra show a single maximum at 520 nm in aqueous medium. This absorption band results when the incident photon frequency is resonant with the collective oscillation of the conduction band electrons and is known as the SPR [30, 31].

Figure 3a(b–d) shows the extinction spectra of substrates after the immobilization of nanoparticles for different soaking times (3, 30, and 60 min) in the colloidal solution of AuNPs. The extinction spectrum contains two bands. The first one was pointed at 545 nm and corresponds to isolated AuNPs in the vicinity of the glass substrate. The observed shift from 520 to 545 nm was due to the modification of the surrounding medium. Concerning the second bands (about 660 nm) indicates the interaction of close nanoparticles and results from dipole–dipole interactions. As presented in Fig. 4a, this coupling between nanoparticles likely results from the increase of

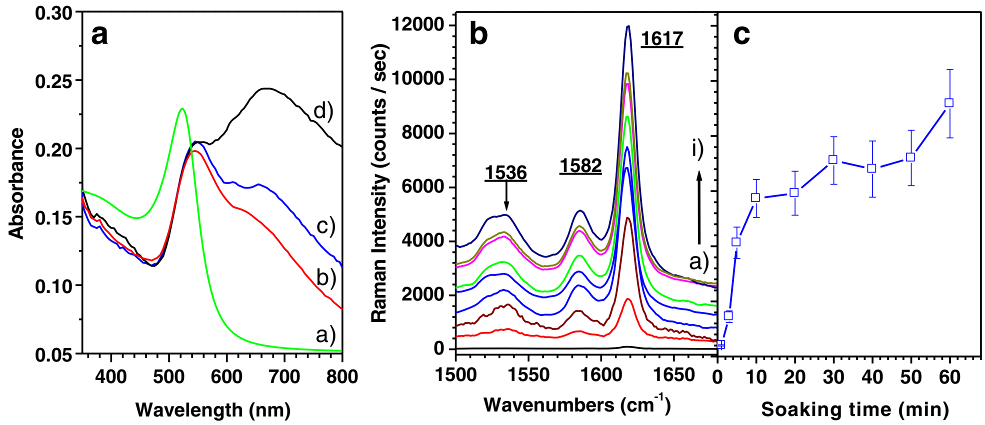

Fig. 3 **a** Extinction spectra of AuNPs (mean diameter of about 22 nm) in water (*a*) and electrostatically adsorbed on APDMES-coated glass as a function of the soaking time of the substrate in a solution of AuNPs [(*b*) 3 min, (*c*) 30 min, (*d*) 60 min]. **b** SERS spectra recorded on a substrate dipped in a 1-μM crystal violet aqueous solution (*a*–*i*): 0, 3, 5, 10, 20, 30, 40, 50, and 60 min, respectively; **c** Raman intensity of the band at 1,620 cm^{-1} of crystal violet as a function of the soaking time of the substrate in the colloidal solution. The acquisitions of data were repeated (five to ten Raman spectra for each experimental condition in our present study) at different locations in order to give a full statistical understanding of the enhancement factor. The intensity was deducted from the baseline in **b**

the density of nanoparticles on the surface (from 300 to 800 AuNPs/μm^2). In consequence, from a rough approximation, we estimated that the mean inter-AuNPs of distance decreased from 35 to 14 nm, as illustrated in Fig. 4b. It should be pointed here that these numerical values were estimated from SEM images (see Fig. S3 in complementary materials). The calculations of density were performed five times for each experimental condition and at different locations.

Raman enhancement measurements

SERS spectra of crystal violet adsorbed from the dye 1 μM aqueous solution on the Au colloidal film were registered with a 676.4-nm excitation in the 1,500 to 1,700 cm^{-1} range (Fig. 3b). The SERS intensity varied appreciably with the soaking time, the density, and the distance between AuNPs immobilized on the substrates. Here, we focused our attention on the C–C in-plane stretching mode observed at 1,620 cm^{-1} [32].

Figure 3c shows the enhancement intensity as a function of the density of AuNPs adsorbed on the substrates (immersion time in the colloidal solution of AuNPs, see Fig. 4). The Raman intensity increases strongly at first and slower after 10 min of soaking time. Thus, as expected, gold surfaces with periodic nanoscale features enhance the Raman scattering. Indeed, the increase of the density of particles on the surface and the decrease of the distance between them enhances the local electromagnetic field and Raman scattering [18, 33]. Accordingly, we assume that the number of locations of “hot spots” grows, which leads to observe strong Raman scattering signals. Likely, the increased number of adsorbed AuNPs is not the only/main parameter leading to higher Raman signal. As we can see in Fig. 3a, the increased number of adsorbed AuNPs induced a new absorption band around 660 nm. It could be stressed here that this absorption band was close to the excitation wavelength used in the Raman experiments (λex=676.4 nm). The correlation between the SERS intensity and the LSPR band at ca. 660 nm confirms once more the importance to optimize the experimental condition in this type of spectroscopy in order to simultaneously benefit of all enhancing parameters.

e-Beam nanopatterned substrates

In the first part of our work, we studied the impact of the interparticle distances of few nanometers which is the most important parameter to optimize for SERS efficiency (when the NP size is fixed). In order to obtain a best control on the regularity and on the reproducibility, thanks to the e-beam nanolithography, we have developed different subtracts with various patterns. We have chosen two kinds of patterns, lines and circles. The interline and inter-circle distances were set from 20 to 2,000 nm. Two line thickness values, 30 and 60 nm, had been achieved, corresponding to bands of two or three AuNP widths. Unfortunately, non-consistent results had been obtained on lines and circles with low interline distances (20 and 40 nm). So, we decided to suppress values concerning them. It should be pointed here that “line” patterns were sensitive to the light polarization, whereas “circle” patterns were nonsensitive.

Considering the preliminary study presented above, we chosen to immerse the nanopatterned samples for 30 min in the AuNP solution. In Fig. 5a–d, AFM and SEM images showing two examples of surface prepared by the method of controlled adsorption are presented. Observations show that the nanoparticles are deposited preferentially on the silanized patterns. The widths of the AuNP lines are the same order of magnitude as the patterns of the masks of PMMA. About three

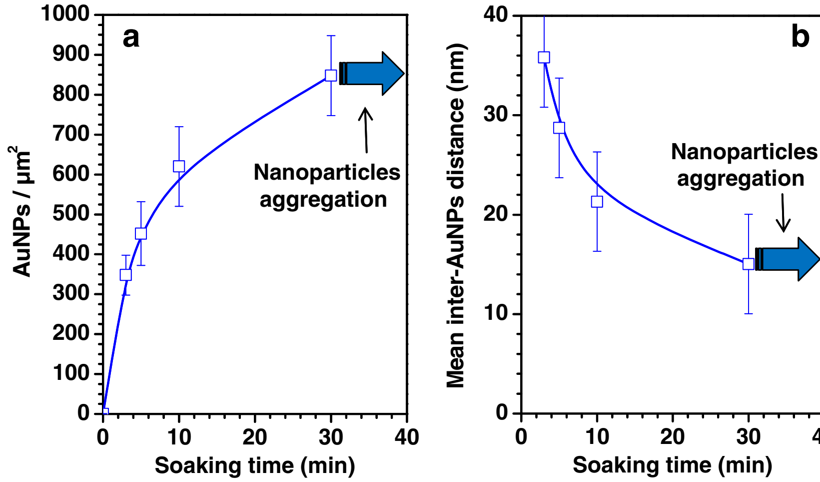

Fig. 4 **a** Density of AuNPs on the APDMES-coated glass as a function of the soaking time. Values were estimated from FE-SEM images (see supplementary materials). The measures of density were performed five times for each experimental condition and at different locations (each measure on a 1-µm^2 area). **b** Mean interparticle distances estimated from FE-SEM image and rough calculation (based on a regular hexagonal arrangement of nanoparticles)

or four nanoparticles were arranged on the line width. In these regions, the height profiles are in the order of magnitude of diameters of nanoparticles in solution. This suggests that a monolayer of nanoparticles was adsorbed.

Figure 5e displays experimental Raman scattering results obtained on various patterns. The intensity (counts/s) of the band at 1,620 cm^{-1} (crystal violet) is reported as a function of the distance interlines. It should be noted that the intensity of Raman scattering varied significantly depending on the pattern. Signals recorded on concentric rings were lower than observed for lines in agreement with simple light polarization considerations.

We can highlight the effectiveness of patterns of lines separated by 60 nm. On these surfaces, the enhancement can be explained by tightening of the lines and the larger number of lines in the analysis surface. This observation is supported by the pattern where the lines are separated by 2 µm. In this case, the diameter of the incident laser beam is about 2 µm, and only one or two lines were involved in the Raman experiments. The number of hot spots is limited (compared to other patterns), and therefore, we observe a low intensity of the Raman signal. However, no significant effect was demonstrated when spacing was beyond 40 nm. This observation confirms that the SERS experiments require that gold diffusers have to be very close and 40 nm is already a lot.

Conclusions

Immobilization of rather regular 2D nanostructures of AuNP was obtained on a APDMES-coated glass or silicon substrates with different soaking time in an AuNPs aqueous solution at 40 °C. Density and mean interparticle distances change as a function of soaking times were studied by SEM and optical spectroscopy (UV-vis). It was found that the red shift of the absorption is strongly dependent on the nanoparticles distribution on the surface. Then, the SERS activity observed from the gold surfaces was compared after dipping the substrates in

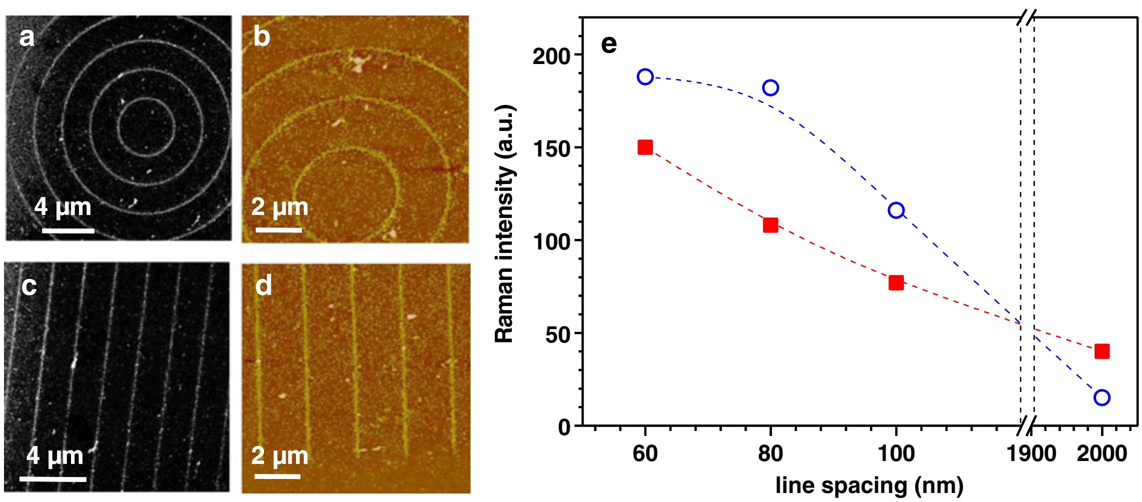

Fig. 5 SEM (**a** and **c**) images and tapping mode AFM images (**b** and **d**) of immobilized AuNPs on nanopatterned substrates (by immersing the substrate in a suspension of AuNPs). **e** Comparison of the Raman intensity measured for the band of crystal violet at 1,620 cm^{-1} as a function of the distance between AuNPs lines (*square* : 30 nm width of the line, *circle* : 60 nm width of the lines)

a 1-μM crystal violet aqueous solution. The SERS intensity varied significantly with the change in the nanoparticle density adsorbed on the substrates. The reasons for these changes were assigned to the distance inter-particles and the correlation between the experimental condition and the LSPR. Finally, controlled gold nanostructures on nanopatterned silicon substrates have been made. The followed method allowed the preparation for structured substrates with good resolution (patterns width inferior to 100 nm). The analysis of Raman spectra of crystal violet set down on these surfaces tends to demonstrate the influence of tightening the lines of each pattern. However, no effect had been put in evidence when interline was beyond 40 nm. From this work, we have tried to demonstrate experimentally that to observe a significant enhancement by SERS, the gold diffusers must be extremely closer. In this context, electron beam lithography will be a very competitive and attractive technique for the realization of SERS substrate if it allows to perform regular patterns separate of less than 20 nm.

Acknowledgments We thank Victor Le Nader at IMN for the helpful discussions.

References

1. Aroca R (2006) Surface-enhanced vibrational spectroscopy. Wiley, Chichester
2. Bell SEJ, Sirimuthu NMS (2008) Quantitative surface-enhanced Raman spectroscopy. Chem Soc Rev 37:012–1024. doi:10.1039/B705965P
3. Louis C, Pluchery O (2012) Gold nanoparticles for physics, chemistry and biology. Imperial College, London, p 395
4. Creighton JA, Blatchford CG, Albrecht MG (1979) Plasma resonance enhancement of Raman scattering by pyridine adsorbed on silver or gold sol particles of size comparable to the excitation wavelength. J Chem Soc Faraday Trans 75:790–798. doi:10.1039/F29797500790
5. Novotny L, Hecht B (2006) Principles of nano-optics. Cambridge University, Cambridge
6. Schlegel VL, Cotton TM (1991) Silver-island films as substrates for enhanced Raman scattering: effect of deposition rate on intensity. Anal Chem 63:241–247. doi:10.1021/ac00003a010
7. Abu Hatab NA, Oran JM, Michael Sepaniak MJ (2008) Surface-enhanced Raman spectroscopy substrates created via electron beam lithography and nanotransfer printing. ACS Nano 2:377–385. doi:10.1021/nn7003487
8. Zrimsek AB, Henry A-I, Van Duyne RP (2013) Single molecule surface-enhanced Raman spectroscopy without nanogaps. J Phys Chem Lett 4:3206–3210. doi:10.1021/jz4017574
9. Zhu T, Yu HZ, Wang J, Wang YQ, Cai SM, Liu ZF (1997) Two-dimensional surface enhanced Raman mapping of differently prepared gold substrates with an azobenzene self-assembled monolayer. Chem Phys Lett 265:334–340
10. Zheng J, Zhu Z, Chen H, Liu Z (2000) Nanopatterned assembling of colloidal gold nanoparticles on silicon. Langmuir 16:4409–4412. doi:10.1021/la991332o
11. Baibarac M, Mihut L, Louarn G, Lefrant S, Baltog Y (2000) Doping and metallic-support effect evidenced on SERS spectra of polyaniline thin films. J Polym Sci Polym Phys 38:2599–2609. doi:10.1002/1099-0488(20001001)38:19<2599::AID-POLB120>3.0.CO;2-Y
12. Li X, Xu W, Zhang J, Jia H, Yang B, Zhao B, Ozaki Y (2004) Self-assembled metal colloid films: two approaches for preparing new SERS active substrates. Langmuir 20:1298–1304. doi:10.1021/la035639
13. Maury P, Escalante M, Reinhoudt DN, Huskens J (2005) Directed assembly of nanoparticles onto polymer- imprinted or chemically patterned templates fabricated. Adv Mater 17:2718–2723. doi:10.1002/adma.200501072
14. Wang H, Levin CS, Halas NJ (2005) Nanosphere arrays with controlled sub-10-nm gaps as surface-enhanced Raman spectroscopy substrates. J Am Chem Soc 127:14992–14993. doi:10.1021/ja055633y
15. Toderas F, Baia M, Baia L, Astilean S (2007) Controlling gold nanoparticle assemblies for efficient surface-enhanced Raman scattering and localized surface plasmon resonance sensors. Nanotechnology 18:255702. doi:10.1088/0957-4484/18/25/255702
16. Hossain MK, Shibamoto K, Ishioka K, Kitajima M, Mitani, Nakashima S (2007) 2D nanostructure of gold nanoparticles: an approach to SERS-active substrate. J Lumin 122:792–795. doi:10.1016/j.jlumin.2006.01.290
17. Wang Y, Chen H, Wang E (2008) Facile fabrication of gold nanoparticle arrays for efficient surface-enhanced Raman scattering. Nanotechnology 318(1):82–7. doi:10.1088/0957-4484/19/10/105604
18. Konrad MP, Doherty AP, Bell SEJ (2013) Stable and uniform SERS signals from self-assembled two-dimensional interfacial arrays of optically coupled Ag nanoparticles. Anal Chem 85:6783–6789. doi:10.1021/ac4008607
19. Hajduková N, Procházka M, Štěpánek J, Špírková M (2007) Chemically reduced and laser-ablated gold nanoparticles immobilized to silanized glass plates: preparation, characterization and SERS spectral testing. Colloids Surf A 301:264–270. doi:10.1016/j.colsurfa.2006.12.065
20. Grausem J, Humbert B, Spajer M, Courjon D, Burneau A, Oswalt J (1999) Near-field Raman spectroscopy. J Raman Spectrosc 30:833–840. doi:10.1002/(SICI)1097-4555(199909)30:9<833::AID-JRS455>3.0.CO;2-#
21. Turkevich J, Stevenson PC, Hillier J (1951) A study of the nucleation and growth processes in the synthesis of colloidal gold. Discuss Faraday Soc 11:55–75. doi:10.1039/DF9511100055
22. Frens G (1972) Controlled nucleation for the regulation of the particle size in monodisperse gold suspensions. Nature 241:20–22. doi:10.1038/physci241020a0
23. Haiss W, Thanh NTK, Aveyard J, Fernig DG (2007) Determination of size and concentration of gold nanoparticles from UV-vis spectra. Anal Chem 79:4215–4221. doi:10.1021/ac0702084
24. Pallandre A, Glinel K, Jonas AM, Nysten B (2004) Binary nanopatterned surfaces prepared from silane monolayers. Nano Lett 4:365–371. doi:10.1021/nl035045n
25. Baralia GG, Pallandre A, Nysten B, Jonas AM (2006) Nanopatterned self-assembled monolayers. Nanotechnology 17:1160. doi:10.1088/0957-4484/17/4/053
26. Shipway AN, Katz E, Willner I (2000) Nanoparticle arrays on surfaces for electronic, optical, and sensor applications. Chem Phys Chem 1:18–52. doi:10.1002/1439-7641(20000804)1:1<18::AID-CPHC18>3.0.CO;2-L
27. Grabar KC, Allison KJ, Baker BE (1996) Two-dimensional arrays of colloidal gold particles: a flexible approach to macroscopic metal surfaces. Langmuir 12:2353–2361. doi:10.1021/la950561h

28. Grabar KC, Freeman RG, Hommer MB, Natan MJ (1995) Preparation and characterization of Au colloid monolayers. Anal Chem 67:735–743. doi:10.1021/ac00100a00
29. Pazos-Perez N, Ni W, Schweikart A, Alvarez-Puebla RA, Fery A, Liz-Marzan LM (2010) Highly uniform SERS substrates formed by wrinkle-confined drying of gold colloids. Chem Sci 1:174–178. doi:10.1039/C0SC00132E
30. Basu S, Kumar Ghosh S (2007) Biomolecule induced nanoparticle aggregation: effect of particle size on interparticle coupling. J Colloid Interface Sci 313:724–734. doi:10.1016/j.jcis.2007.04.069
31. Makiabadi T, Bouvrée A, Le Nader V, Terrisse H, Louarn G (2010) Preparation, optimization and characterization of SERS sensor substrates based on two dimensional structures of Au colloid. Plasmonics 5:21–29. doi:10.1007/s11468-009-9110-6
32. Canamares MV, Chenal C, Birke RL, Lombardi JR (2008) DFT, SERS, and single-molecule SERS of crystal violet. J Phys Chem C 112:20295–20300. doi:10.1021/jp807807j
33. Campion A, Kambhampati P (1998) Surface-enhanced Raman scattering. Chem Soc Rev 27:241–250. doi:10.1039/A827241Z